

000 001 002 003 004 005 006 007 IT HEARS, IT SEES TOO: MULTI-MODAL LLM FOR 008 DEPRESSION DETECTION BY INTEGRATING VISUAL 009 UNDERSTANDING INTO AUDIO LANGUAGE MODELS 010 011

012 **Anonymous authors**
013

014 Paper under double-blind review
015
016
017
018
019
020
021
022
023
024
025
026
027
028
029

030 ABSTRACT 031

032 Depression is one of the most prevalent mental health disorders globally. In recent
033 years, multi-modal data, such as speech, video, and transcripts, has been increasing-
034 ly used to develop AI-assisted depression assessment systems. Large language
035 models have further advanced this field due to their strong language understanding
036 and generalization capabilities. However, conventional LLMs remain text-centric
037 and cannot process the rich non-verbal cues found in audio and visual modalities,
038 which are critical components in mental health evaluation. While multi-modal
039 LLMs offer a promising direction, few are tailored for psychological applications.
040 In this study, we propose a novel multi-modal LLM framework for depression de-
041 tection. Our approach augments an audio language model with visual under-
042 standing and aligns audio-visual features at the timestamp level. This fine-grained align-
043 ment improves modeling of temporal dynamics across modalities while reducing
044 the need for extensive training data and computational resources. Experiments
045 on the DAIC-WoZ dataset demonstrate that our model outperforms both single-
046 modality approaches and previous multi-modal methods. Moreover, the proposed
047 framework can be extended to incorporate additional physiological signals, paving
048 the way for broader clinical applications beyond mental health.
049

050 1 INTRODUCTION 051

052 Depression has emerged as a critical concern in the field of mental health, affecting a broad pop-
053 ulation across various age groups. Particularly, the incidence of depression among adolescents has
054 surged over the past decade, raising significant social and public health concerns (Thapar et al.,
055 2022). Diagnosing and treating depression often entails substantial labor and financial costs for
056 both families and healthcare systems. With the advancement of natural language processing (NLP),
057 increasing attention has been given to automated approaches for depression detection, reducing hu-
058 man intervention. Large language models (LLMs) have demonstrated remarkable capabilities across
059 a wide array of NLP tasks (Naveed et al., 2023), which has sparked interest in their application to
060 mental health screening (Hengle et al., 2024; Xu et al., 2024). Despite their success, a fundamen-
061 tal limitation of conventional LLMs lies in their confinement to textual inputs, lacking the capacity
062 to interpret multi-modal signals such as speech and facial expressions that are also indicative of
063 depressive symptoms (Koops et al., 2023; Krause et al., 2021).
064

065 Multi-modal data, including acoustic and visual cues, can significantly enhance the accuracy of de-
066 pression detection. Prior studies have shown that individuals at high risk of depression often exhibit
067 reduced facial expressiveness, diminished vitality, and weakened responses to external stimuli such
068 as decreased eye contact (Perez & Riggio, 2003; Waxer, 1974). Similarly, specific acoustic features,
069 such as monotonous tone, slow speech rate, disfluency, and low vocal energy, have been linked to
070 depressive states (Koops et al., 2023). These behavioral signals offer valuable complementary infor-
071 mation beyond what can be derived from text alone. Multi-modal large language models (MLLMs)
072 offer an ideal solution to the integration of text and multi-modal data, which shows great promise in a
073 lot of downstream tasks (Zhang et al., 2024a). However, current MLLMs face several limitations that
074 hinder their application to depression detection. First, depression detection relies heavily on tempo-
075 ral data such as audio and video, yet most existing MLLMs are limited to static images (Caffagni
076 et al., 2024). Furthermore, due to the relatively small size of depression-related datasets compared to
077

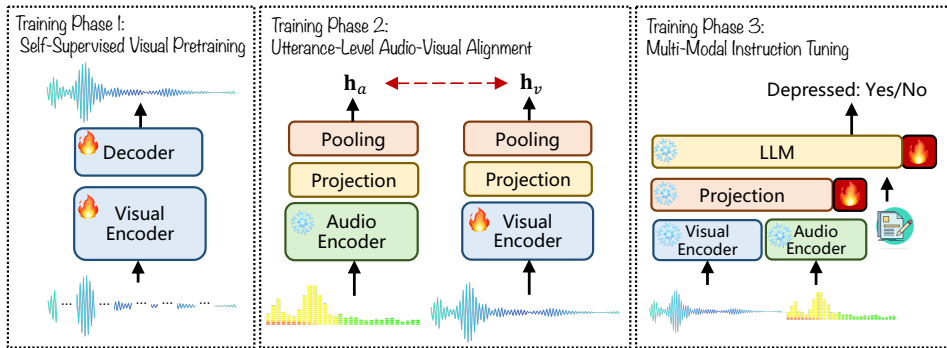


Figure 1: The training scheme of the proposed multi-modal LLM for depression detection.

standard NLP corpora, developing MLLMs for this domain demands careful consideration of model complexity to mitigate overfitting and ensure training efficiency.

To address these limitations, we propose a simple yet effective framework that adapts a multi-modal large language model for depression detection. Our method builds upon a pretrained audio language model (ALM) and augments it with visual understanding capabilities, forming a truly multi-modal system. This design leverages the shared temporal structure of audio and visual modalities, allowing for the alignment at the timestamp level. By incrementally integrating visual modules into the ALM with self-supervised visual pretraining and parameter-efficient fine-tuning (PEFT) (Hu et al., 2022), our approach maintains the efficiency and modularity of the base model while enhancing its multi-modal capacity. This strategy also reduces the number of trainable parameters and mitigates the need for large-scale pretraining, making it efficient in data usage and computational requirements. Experiments on the public depression detection dataset, DAIC-WoZ, confirm the effectiveness of our approach, highlighting its potential for practical applications in mental health assessment.

In summary, the contributions of this work consist of the following aspects:

- We develop a multi-modal large language model for depression detection based on the Qwen2-Audio (Chu et al., 2024) model by integrating a self-supervised vision encoder with parameter-efficient fine-tuning. To the best of our knowledge, this is the first study to propose **multi-modal depression detection using LLM across text, audio, and video modalities**;
- We implement a timestamp-level alignment strategy that enables fine-grained temporal fusion across modalities. This design leverages the inherent temporal characteristics of both audio and video signals, enhancing the model’s capacity to capture subtle behavioral cues indicative of depression.
- We validate our approach by the comparison with single-modality methods and previous LLM-based state-of-the-art methods on the DAIC-WoZ database (Gratch et al., 2014). The experimental results demonstrate that our approach yields superior performance at a smaller model scale (7B versus 13B), compared with pioneering multi-modal LLMs.

2 RELATED WORKS

2.1 AUTOMATED DEPRESSION DETECTION

Deep learning has been widely adopted for automated depression detection using speech, text, and video modalities. Earlier works focused on single modality, such as self-supervised speech models (Wu et al., 2023), hierarchical acoustic representations (Chen et al., 2022), or mobile speech data (Kim et al., 2023). Visual features like facial expressions and eye movements have also shown promise, with methods leveraging weakly supervised learning (Shangguan et al., 2022), gaze patterns (Zheng et al., 2024), and combined facial-gaze analysis (Stolicyn et al., 2022). Recent studies have explored multi-modal fusion to capture richer cues, incorporating audio, video, and text (Zhang et al., 2024c; Shen et al., 2022; Xue et al., 2024). However, most rely on late fusion strategies without joint pretraining, limiting their ability to fully exploit temporal and semantic correlations across modalities.

108
109

2.2 LARGE LANGUAGE MODELS IN DEPRESSION

110
111
112
113
114
115
116
117
118
119
120
121
122

Large language models have been applied to depression detection due to their strong ability to model long-range dependencies in dialogue, which is an essential feature for analyzing clinical interviews. For example, Liu *et al.* (Liu et al., 2023b) introduced ChatCounselor, which leverages LLMs to assess depressive symptoms and provide mental health support. Other studies have employed LLMs to analyze social media content; Hengle *et al.* (Hengle et al., 2024) constructed a benchmark for depression-stress classification from online posts, while Xu *et al.* (Xu et al., 2024) used LLMs to infer depression status from various web-based sources. Recent efforts have extended LLMs to multi-modal settings for improved diagnostic accuracy. Sadeghi *et al.* (Sadeghi et al., 2024) combined LLMs with facial expression analysis to estimate depression severity, and Zhang *et al.* (Zhang et al., 2024b) incorporated acoustic landmarks into LLMs to build an audio-text model for depression detection. While these approaches demonstrate the potential of LLMs in mental health applications, they remain limited to textual inputs or approximations thereof (e.g., acoustic landmarks). The inability to directly process rich multi-modal signals restricts their overall effectiveness.

123

2.3 MULTI-MODAL LARGE LANGUAGE MODELS

124
125
126
127
128
129
130
131
132
133
134
135
136

Integrating textual inputs with audio and visual modalities represents a major advancement in the development of generative AI. The fusion of LLMs with visual encoders has enabled impressive performance on tasks such as visual dialogue, visual question answering, and image captioning (Liu et al., 2023a; Zhu et al., 2023; Dai et al., 2023; Wang et al., 2024; Lu et al., 2024). Similarly, audio language models have emerged to jointly process speech and text. For instance, Chu *et al.* (Chu et al., 2024) introduced Qwen2-Audio, extending the Qwen2-7B backbone (Qwen et al., 2025), while Ding *et al.* (Ding et al., 2025) proposed Kimi-Audio, which incorporates both discrete acoustic tokens and continuous audio embeddings into an LLM framework. Despite their success, these models are generally not well-suited for mental health applications due to substantial domain gaps in both training data and pretraining objectives. Moreover, most vision-language models lack the capacity to handle continuous video input, further limiting their applicability to tasks such as depression detection, where temporal visual cues are crucial.

137
138

3 METHOD

139
140

3.1 OVERVIEW OF THE FRAMEWORK

141
142
143
144
145
146

We propose a multi-modal large language model (MLLM) for depression detection, constructed upon a pretrained audio language model (ALM) as the backbone. As depicted in Figure 2, the framework consists of three key components: (1) an **audio encoder** that processes raw audio signals and extracts temporal embeddings; (2) a **visual encoder** that receives video frames and produces visual embeddings aligned with the audio stream at the timestamp level; (3) a **large language model** that integrates the audio-visual features along with textual inputs to perform depression classification.

147
148
149
150
151
152
153

The training process is divided into three sequential stages. First, the visual encoder is pretrained using a self-supervised learning strategy inspired by masked autoencoders (He et al., 2022), which enhances its capacity to capture rich visual representations. In the second stage, the visual encoder is fine-tuned on a contrastive alignment task designed to match visual and audio embeddings at the utterance level, thereby improving cross-modal temporal synchronization. Finally, the projection layer and LLM are trained using parameter-efficient fine-tuning (PEFT) techniques to effectively incorporate the visual modality while minimizing additional computational overhead.

154
155

3.2 MODEL COMPONENTS

156
157

3.2.1 AUDIO LANGUAGE MODEL

158
159
160
161

We adopt Qwen2-Audio (Chu et al., 2024) as the foundation of our framework. This model integrates Whisper-large-v3 (Radford et al., 2023) as the audio encoder and Qwen2-7B as the language model. The audio encoder processes raw waveforms resampled to 16 kHz and converts them into 128-channel Mel-spectrograms, with each frame representing a 10 ms segment. These spectrograms are subsequently downsampled via strided convolutions and average pooling, resulting in encoder

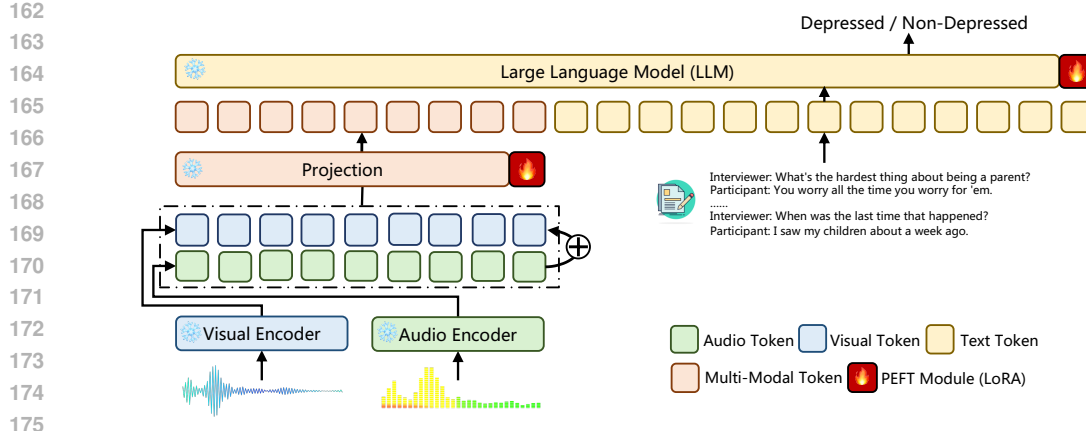


Figure 2: The framework of the proposed multi-modal large language model. The model includes an audio encoder, a visual encoder, and an LLM for detection.

outputs where each frame corresponds to a 40 ms segment of the original waveform. To ensure the universality of our method, we retain the pretrained weights of Qwen2-Audio throughout the initial stages and apply PEFT-based adaptation only in the final training phase. Notably, our framework is modular and can be extended to other audio language models, provided their audio encoders output sequences aligned with fixed temporal intervals.

3.2.2 VISUAL ENCODER

The visual encoder is designed to extract visual embeddings that align temporally with the audio encoder outputs. To ensure architectural compatibility and ease of alignment, its design mirrors the Whisper encoder, comprising a strided convolutional embedding layer, a stack of Transformer encoder layers, and an output average pooling layer. Initially, visual features are resampled to match the temporal resolution of the audio Mel-spectrograms and are projected into the embedding space via 1D convolutions. This embedding process includes striding, reducing the temporal resolution to 20 ms per token. The resulting features are then processed by the Transformer layers and further downsampled through average pooling to match the final 40 ms resolution of the audio encoder outputs. As a result, both audio and visual embeddings are temporally synchronized, as illustrated in Figure 3.

3.2.3 AUDIO-VISUAL PROJECTION

After obtaining audio and visual embeddings, the next step is to fuse them into a unified representation for input into the LLM. While a common fusion strategy involves concatenating modality embeddings along the sequence dimension (Xu et al., 2025), this approach is suboptimal for integrating new modalities into pretrained LLMs, as it disrupts the expected sequence length and can interfere with positional encoding. To preserve compatibility with pretrained LLMs, we propose a simple yet effective fusion method—element-wise addition of audio and visual embeddings, which is illustrated in Figure 2. This is feasible due to our explicit timestamp-level synchronization, ensuring both sequences share the same temporal structure. Moreover, our three-stage training strategy progressively aligns the modalities, enabling effective fusion without representation collapse.

3.3 TIMESTAMP-SYNCHRONIZED DATA AUGMENTATION

Depression corpora typically consist of participant–interviewer interviews, which present two challenges: (1) severe class imbalance, as healthy controls far outnumber depressed individuals, and (2) limited data volume, despite long session durations. To alleviate these issues, we adopt subdialogue shuffling based on Wu et al. (2023), segmenting lengthy interviews into shorter, contiguous exchanges. This increases sample size per participant and enables flexible resampling for class balancing.

Building on Wu et al. (2023), we enhance the method by ensuring timestamp alignment across transcript, audio, and visual modalities. Each subdialogue is constrained to start with an interviewer's

utterance and end with the participant’s response, maintaining contextual coherence and narrowing the domain gap between LLM pre-training and depression detection. We then discard interviewer audio and corresponding visual frames, retaining only participant segments, while preserving interviewer transcripts. This choice reflects two considerations: interviewer speech carries little acoustic value for mental state assessment, yet their utterances are essential for conversational coherence. Although removing interviewer segments inevitably discards some multimodal information, the trade-off between information reduction and coherence is analyzed in Section 4.3.3. Further augmentation details are provided in the Appendix.

3.4 TRAINING

The training pipeline of our framework is divided into three sequential stages, as shown in Figure 1. The first two stages focus on training the visual encoder, while the final stage involves fine-tuning the LLM.

3.4.1 SELF-SUPERVISED VISUAL PRETRAINING

To enhance the visual representation capability of the encoder, we first conduct self-supervised pre-training. Instead of learning directly from raw video data, we opt to pretrain on pre-extracted visual features, as raw video files may contain sensitive content and are often unavailable in commonly used depression-related corpora. This not only addresses potential privacy concerns but also reduces computational overhead, making the approach more generalizable to other time-series modalities such as physiological signals (e.g., rPPG and ECG).

Inspired by the masked autoencoder (MAE) framework (He et al., 2022), we design a reconstruction task where the encoder learns to recover masked portions of the input time series. Specifically, given a sequence input $\mathbf{x} = (x_1, x_2, \dots, x_T) \in \mathbb{R}^{T \times d}$, we randomly mask K frames of the input and use a learnable token $x_{mask} \in \mathbb{R}^d$ shared across all masked frames. The indices for masked tokens are denoted as \mathcal{M} , and the indices for unmasked tokens are denoted as \mathcal{V} . Obviously $\mathcal{V} \cup \mathcal{M} = \{1, 2, \dots, T\}$. The unmasked sequence $\mathbf{x}_{in} = \{x_i | i \in \mathcal{V}\} \in \mathbb{R}^{K \times d}$ are fed to the visual encoder to acquire the latent representation $\mathbf{h} \in \mathbb{R}^{T-K \times d}$. Then, the latent representation \mathbf{h} and masked frames are concatenated together to acquire the input sequence $\mathbf{z} \in \mathbb{R}^{T \times d}$, which are fed to the decoder to obtain the reconstructed input sequence $\hat{\mathbf{x}} \in \mathbb{R}^{T \times d}$. The objective is to minimize the mean squared error (MSE) between the reconstructed and original sequences within the masked regions:

$$\min \frac{1}{|\mathcal{M}|} \sum_{i \in \mathcal{M}} \|\hat{x}_i - x_i\|_2^2 \quad (1)$$

This approach allows the model to capture temporal dependencies and improve robustness in downstream tasks.

3.4.2 UTTERANCE LEVEL AUDIO-VISUAL ALIGNMENT

After the visual pretraining in the first stage, the visual encoder is enabled to extract visual embeddings from input visual feature sequences for downstream tasks. However, the visual comprehension of the visual encoder is not aligned with the audio encoder. To reduce the training gap between both encoders, we design a proxy downstream task with contrastive learning to align the visual encoder with the audio encoder at the utterance level. As illustrated in Figure 3, we add a projection layer to each encoder, respectively, and pool the outputs in the time dimension to obtain the utterance level

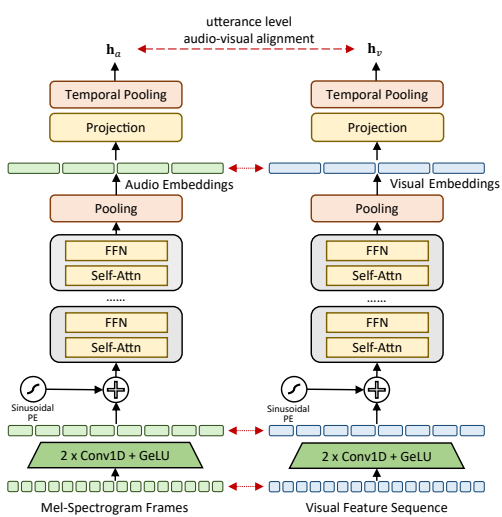


Figure 3: The scheme of utterance-level audio-visual alignment. Audio and visual inputs are strided simultaneously, ensuring synchronization on timestamps.

270 representations. Given a mini-batch of audio outputs $\mathbf{h}_a \in \mathbb{R}^{N \times d}$ and visual outputs $\mathbf{h}_v \in \mathbb{R}^{N \times d}$,
 271 where N denotes the batch size, we obtain a similarity matrix $\mathbf{Sim} = \mathbf{h}_a \mathbf{h}_v^T \in \mathbb{R}^{N \times N}$. The learning
 272 objective is to find the correct match of each audio-visual pair for utterance level audio-visual
 273 alignment:

$$274 \quad \min \mathcal{L}_{ce}(\mathbf{Sim}/\tau, \mathbf{I}_N) \quad (2)$$

275 where \mathcal{L}_{ce} denotes cross-entropy loss, \mathbf{I}_N denotes the identity matrix, and τ is the temperature
 276 parameter.

277 During this stage, we freeze the entire audio encoder and the lower layers of the visual encoder to
 278 preserve the representations learned in the initial stage. Only the upper layers of the visual encoder
 279 receive gradient updates, ensuring stability and preventing catastrophic forgetting.

281

282 3.4.3 MULTI-MODAL INSTRUCTION TUNING

283

284 In the final stage, we integrate the pretrained visual encoder with the audio language model to con-
 285 struct a multi-modal large language model tailored for depression detection, which is illustrated in
 286 Figure 2. Since traditional LLMs are not inherently designed to process visual information, addi-
 287 tional instruction tuning is required to adapt the model to this task. We employ Low-Rank Adap-
 288 tation (LoRA) (Hu et al., 2022) to update the parameters of both the LLM and the modality projec-
 289 tion layer. As audio and visual features have been temporally synchronized and aligned at the utterance
 290 level in previous stages, the complexity of cross-modal fusion is substantially reduced.

291

292 3.5 MULTI-SCALE SLIDING-WINDOW INFERENCE

293

294 Since our model is trained on subdialogues rather than entire conversations, we adopt a multi-scale
 295 sliding-window inference strategy to derive a final prediction for each full conversation. This ap-
 296 proach aggregates predictions from multiple subdialogue segments extracted at different temporal
 297 scales. Specifically, for each conversation, we generate a fixed number (200) of subdialogues at three
 298 predefined durations: 30s, 75s, and 120s. This multi-scale design ensures that each temporal reso-
 299 lution contributes equally to the final decision, capturing both short-term and long-term behavioral
 300 cues. The overlap between adjacent subdialogues is dynamically adjusted based on the conversa-
 301 tion length and the total number of segments per setting. Each time-scale configuration yields an
 302 independent conversation-level prediction, and the final prediction is determined by majority voting
 303 across the three settings.

304

305 4 EXPERIMENTS

306

307 4.1 DATABASE AND IMPLEMENTATION DETAILS

308

309 We utilize the DAIC-WoZ database (Gratch et al., 2014), one of the most popular datasets for depres-
 310 sion detection, to develop and evaluate our proposed multi-modal LLM in depression detection. The
 311 DAIC-WoZ database contains interview transcripts, speech records, and visual features from 189
 312 participants, including healthy controls and depression cases. The golden labels of the dataset are
 313 based on PHQ-8 scores, where a PHQ-8 score higher than 10 is recognized as a depressed case. The
 314 training set contains 107 participants, 30 of whom are labeled as depressed, while the development
 315 set contains 35 participants, 12 of whom are labeled as depressed. Following our previous works (Wu
 316 et al., 2023; Zhang et al., 2024b), we report the evaluation results on the development set for compar-
 317 ison. In addition to the training set and development set, we also evaluated our method on the test set,
 318 where 14 out of the 47 subjects are labeled as depressed. For timestamp-synchronized data augmen-
 319 tation, we set the maximum length of each subdialogue to 120 seconds, generate 1,000 subdialogues
 320 per conversation with depression, which achieves a trade-off between data diversity and the risk of
 321 overfitting. The visual features generated by data augmentation are utilized for self-supervised vi-
 322 sual pretraining and utterance level audio-visual alignment. Then the augmented transcripts, audio
 323 clips, and visual features are used for multi-modal instruction finetuning. Our multi-modal LLM for
 depression detection is developed on Qwen2-Audio-7B-Instruct model. We utilize 2 NVIDIA H200
 141G GPUs during training. The detailed training hyperparameters have been demonstrated in the
 Appendix.

324 4.2 RESULTS
325

326 We compare our methods with previous methods, including single-modal approaches, conventional
327 multi-modal approaches, and multi-modal LLMs, on both the development set and test set of the
328 DAIC-WoZ database. The detailed comparison results are illustrated in Table 1, Table 2, and Table
329 3, respectively. Following previous works, we adopt the F1 score for evaluation.

330 **Evaluation on DAIC-WoZ Dev Set** We present a comprehensive comparison between our proposed multi-modal LLM
331 and previous methods on the DAIC-WoZ development set in
332 Table 1. Additionally, we evaluate the contribution of each individual module in our framework, including the Qwen2-7B
333 model, the Whisper-v3 audio encoder, and a self-supervised
334 vision encoder. Overall, our multi-modal model achieves superior
335 classification performance on the development set of the
336 DAIC-WoZ dataset, consistently outperforming all single-
337 modality baselines.

338 Text-based models show that Llama2-13B (Touvron et al.,
339 2023; Zhang et al., 2024b) performs best among text-only
340 models, likely due to its larger parameter scale. Among
341 smaller models, Qwen2-7B and Llama2-7B exhibit similar
342 performance but fall short of the 13B variant. Interestingly,
343 GPT-4, despite its scale and zero-shot capabilities, underper-
344 forms relative to Llama2-13B. Likewise, RoBERTa surpasses
345 GPT-4 despite its significantly smaller size as well. A simi-
346 lar phenomenon has been observed in Zhang et al. (2024b).
347 This performance gap may be attributed to the nature of de-
348 pression detection, which emphasizes representation learn-
349 ing over generative modeling, making encoder-based models
350 more suitable.

351 Audio-based models generally outperform text-only models,
352 suggesting that acoustic cues carry richer information for de-
353 tecting depressive symptoms. In addition, the performance of
354 audio models could benefit from downstream tasks such as speech
355 recognition (Wu et al., 2023). Notably, WavLM fine-tuned for emotion
356 recognition, surpassing even Whisper-v3-large. This suggests that tasks closely related to depression,
357 such as emotion recognition and ASR, provide transferable knowledge useful for this application.

358 For video models, our finetuned visual encoder with a classifica-
359 tion head achieves the best performance. The main factor that could affect video-based models is the choice of visual feature sets.
360 Since raw videos are not available at the DAIC-WoZ database, only facial feature sets, such as land-
361 marks and action units, are available for depression detection. As the feature set could be rather
362 redundant, the performance of video models could even deteriorate if the feature set selection is
363 inappropriate. Self-supervised pretraining alleviates the issue significantly, as masked autoencoders
364 are designed for images, which possess a redundant nature, and are suitable in our scenario.

365 Multi-modal approaches that incorporate both audio and text, or integrate all three modalities, gen-
366 erally outperform single-modal baselines. In particular, the inclusion of audio features often leads
367 to significant performance improvements, highlighting the importance of acoustic information in
368 depression detection. Compared with other multi-modal methods, our proposed framework con-
369 sistently achieves superior results, demonstrating the effectiveness of timestamp-level alignment and
370 the synergy of modality-specific encoders in capturing clinically relevant cues.

371 **Comparison with Multi-Modal LLMs** Table 2 presents the performance comparison between
372 our method and existing multi-modal LLMs. Together with Table 1, the results demonstrate that
373 incorporating audio significantly enhances the classification performance of LLMs. For instance,
374 augmenting Llama2-13B with acoustic landmarks improves its F1 score from 0.636 to 0.695. A
375 similar trend is observed with Qwen2-7B, where the inclusion of audio elevates the F1 score from
376 0.578 to 0.720. Our proposed multi-modal framework, which jointly models text, audio, and vi-

Modality	Models	F1
Text	RoBERTa 2022	0.602
	Llama2-7B 2024b	0.578
	Llama2-13B 2024b	0.636
	Qwen2-7B 2024	0.564
	GPT4 2024b	0.571
Audio	HuBERT 2023	0.640
	WavLM 2023	0.720
	SpeechFormer 2022	0.694
	SpeechFormer++ 2023	0.709
	Whisper-v3 2023	0.694
Video	GSM 2016	0.530
	SSL + CLS	0.668
A+T	AudiBERT 2021	0.709
	TOAT 2022	0.741
	LSTM 2018	0.770
A+T+V	C-CNN 2018	0.769
	ConvBiLSTM 2022	0.70*
	Ours w/o MS	0.789
	Ours	0.844

Table 1: The performance comparison of our method and other approaches on DAIC-WoZ development set. “*” denotes that the original results are reported with 2 significant digits. “MS” denoting the multi-scale strategy in our inference.

sual signals, achieves the highest F1 score of 0.789, validating the benefit of integrating visual cues alongside audio and language inputs. This underscores the advantage of leveraging complementary modalities for capturing the complex and multi-faceted nature of depressive symptoms. Notably, both our approach and Qwen2-Audio variants outperform LLMs with acoustic landmarks, despite relying on smaller language backbones (7B vs 13B). This suggests that native multi-modal architectures might be more adept at interpreting raw sensory inputs. While acoustic landmarks serve as a lightweight representation of audio, they may omit subtle prosodic or emotional cues that are preserved in the original waveforms. In contrast, models trained end-to-end on raw audio exhibit stronger modality comprehension and more effective feature fusion.

Evaluation on DAIC-WoZ Test Set In addition, since the golden labels of the DAIC-WoZ test set have been released, we compare our method with previous state-of-the-art approaches on this benchmark. The quantitative results are presented in Table 3. It can be observed that single-modal approaches yield similar or slightly lower F1 scores on the test set compared to their performance on the development set. In contrast, a recent multi-modal approach that integrates audio, video, and textual information (Jung et al., 2024) achieves significantly better results than single-modal methods. Overall, our method outperforms both previous single-modal and multi-modal approaches on the test set, demonstrating its effectiveness and robustness.

Model	Base Model	F1
(Zhang et al., 2024b)	7B	0.545
	7B-Chat	0.500
	13B	0.695
	13B-Chat	0.666
(Chu et al., 2024)	7B	0.650
	7B-Instruct	0.720
Ours w/o audio	7B	0.617
	7B-Instruct	0.643
Ours	7B	0.709
	7B-Instruct	0.789

Table 2: The performance comparison of our method and multi-modal LLMs on DAIC-WoZ development set. Note that for fair comparison we do not employ model ensemble or multi-scale inference.

Models	Modality	F1
GloVe-CNN (Campbell et al., 2022)	Text	0.68*
TOAT (Guo et al., 2022)	Audio	0.647
EmoAudioNet (Othmani et al., 2021)	Audio	0.66*
HiQuE (Jung et al., 2024)	A+T+V	0.79*
Ours	A+T+V	0.825

Table 3: The performance comparison of our method and previous approaches on DAIC-WoZ test set. “*” denotes that the original results are reported with 2 significant digits.

4.3 ABLATION STUDIES AND DISCUSSION

In this section, we analyze the source of performance gain in our framework, including the contribution of each modality and the selection of the base model. In addition, we discuss the effectiveness of our proposed timestamp-synchronized data augmentation upon the removal of the interviewer’s utterance and context length in subdialogues. The experiments are all conducted on the development set of DAIC-WoZ.

4.3.1 THE CONTRIBUTION OF EACH MODALITY

We further investigate the individual contribution of each modality within our framework. As shown in Table 1, both audio and video modalities enhance depression detection performance. The baseline Qwen2-7B model achieves an F1 score of 0.564 using text alone. Introducing audio features leads to a substantial improvement, raising the F1 score to 0.720. Further incorporation of video features elevates the performance to 0.789. Additionally, our proposed multi-scale sliding-window strategy contributes to model performance significantly, improving the F1 score to 0.844.

An interesting observation is that the addition of audio yields a greater performance gain compared to the inclusion of video, in both instruction-tuned and pre-trained variants. This discrepancy can be attributed to two primary factors. First, as pre-extracted visual features rather than raw video data are utilized in our framework, the model may face information loss, leading to reduced expressive power. Second, our model is fundamentally built upon an audio language modeling architecture. Removing

432 audio embeddings may disrupt the alignment mechanism across modalities, thereby compromising
 433 the model’s ability to integrate non-verbal cues effectively.
 434

435

436 4.3.2 THE CHOICE OF BASE MODEL 437

438 Since both pretrained model and instruction-tuned model are available in Qwen2-Audio families,
 439 we compare the performance of these two model variants as the base model. The results in Table
 440 2 indicate that the instruction-tuned model provides higher detection performance. The findings in
 441 our research are different from previous work (Zhang et al., 2024b), where instruction tuning leads
 442 to significant performance deterioration compared with the pretrained model. The reasons for the
 443 inconsistency could be the difference in instruction tuning in general LLMs and audio language
 444 models. Depression detection involves the analysis of both audio and text; a similar task has been
 445 used to finetune the model in instruction tuning. Thus, the instruction-tuned model could be better
 446 at the audio analysis task.
 447

448

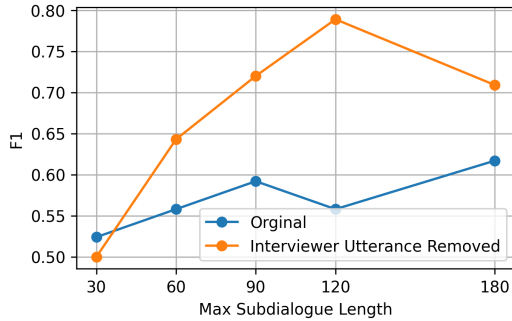
449 4.3.3 THE EFFECT OF CONTEXT LENGTH AND INTERVIEWER UTTERANCE REMOVAL 450

451 The length of subdialogues plays a crucial role
 452 in our framework, as longer contexts gener-
 453 ally provide richer cues for depression detec-
 454 tion. However, longer subdialogues do not nec-
 455 essarily improve the performance for detec-
 456 tion, as the audio records for the interviewer
 457 do not contribute to the decision, but even in-
 458 terfere with the depression detection. To ad-
 459 dress this constraint, we propose to remove the
 460 interviewer’s utterances during data augmenta-
 461 tion, allowing more content from the partici-
 462 pант to be retained within the fixed audio win-
 463 dow. While this enhances the availability of
 464 participant-specific acoustic cues, it also results
 465 in the loss of visual information associated with
 466 the removed segments. To explore this trade-
 467 off, we conduct an ablation study under vary-
 468 ing subdialogue lengths, as shown in Figure 4. When
 469 the maximum subdialogue length is constrained to 30 sec-
 470 onds, removing the interviewer’s speech
 471 leads to degraded performance. In this setting, the entire subdialogue can be encoded without trun-
 472 cation, and discarding the interviewer’s turns causes unnecessary loss of visual cues, thus impairing
 473 multi-modal inference. In contrast, as the subdialogue length increases beyond the model’s audio
 474 capacity, the removal of interviewer utterances proves beneficial. By prioritizing participant speech
 475 within the fixed input window, the model gains access to more relevant acoustic information, leading
 476 to improved detection accuracy. However, when the context length becomes excessively long, the
 477 performance gain diminishes. This is likely due to reduced dialogue diversity and increased risk of
 478 overfitting, as longer subdialogues tend to be less variable.
 479

480 5 CONCLUSION 481

482

483 In this study, we propose a multi-modal large language model for depression detection, built upon
 484 audio-based language models and augmented with visual understanding capabilities. Experiments
 485 on the DAIC-WoZ dataset demonstrate the superiority of our framework over existing multi-modal
 486 LLMs. To our knowledge, this is the first work to develop a multi-modal LLM for depression detec-
 487 tion that simultaneously integrates textual, audio, and visual modalities. We further provide detailed
 488 analyses of how model design and data augmentation strategies affect performance. Overall, our
 489 method offers an effective solution for adapting multi-modal LLMs to mental health applications,
 490 with potential for broader extension to other domains.
 491



492 Figure 4: The depression detection performance
 493 on subdialogue length with or without inter-
 494 viewer’s utterances.

495

496

497

498

499

500

501

502

503

504

505

506

507

508

509

510

511

512

513

514

515

516

517

518

519

520

521

522

523

524

525

526

527

528

529

530

531

532

533

534

535

536

537

538

539

540

541

542

543

544

545

546

547

548

549

550

551

552

553

554

555

556

557

558

559

560

561

562

563

564

565

566

567

568

569

570

571

572

573

574

575

576

577

578

579

580

581

582

583

584

585

586

587

588

589

590

591

592

593

594

595

596

597

598

599

600

601

602

603

604

605

606

607

608

609

610

611

612

613

614

615

616

617

618

619

620

621

622

623

624

625

626

627

628

629

630

631

632

633

634

635

636

637

638

639

640

641

642

643

644

645

646

647

648

649

650

651

652

653

654

655

656

657

658

659

660

661

662

663

664

665

666

667

668

669

670

671

672

673

674

675

676

677

678

679

680

681

682

683

684

685

686

687

688

689

690

691

692

693

694

695

696

697

698

699

700

701

702

703

704

705

706

707

708

709

710

711

712

713

714

715

716

717

718

719

720

721

722

723

724

725

726

727

728

729

730

731

732

733

734

735

736

737

738

739

740

741

742

743

744

745

746

747

748

749

750

751

752

753

754

755

756

757

758

759

760

761

762

763

764

765

766

767

768

769

770

771

772

773

774

775

776

777

778

779

780

781

782

783

784

785

786

787

788

789

790

791

792

793

794

795

796

797

798

799

800

801

802

803

804

805

806

807

808

809

810

811

812

813

814

815

816

817

818

819

820

821

822

823

824

825

826

827

828

829

830

831

832

833

834

835

836

837

838

839

840

841

842

843

844

845

846

847

848

849

850

851

852

853

854

855

856

857

858

859

860

861

862

863

864

865

866

867

868

869

870

871

872

873

874

875

876

877

878

879

880

881

882

883

884

885

886

887

888

889

890

891

892

893

894

895

896

897

898

899

900

901

902

903

904

905

906

907

908

909

910

911

912

913

914

915

916

917

918

919

920

921

922

923

924

925

926

927

928

929

930

931

932

933

934

935

936

937

938

939

940

941

942

943

944

945

946

947

948

949

950

951

952

953

954

955

956

957

958

959

960

961

962

963

964

965

966

967

968

969

970

971

972

973

974

975

976

977

978

979

980

981

982

983

984

985

986

987

988

989

990

991

992

993

994

995

996

997

998

999

999

486 REFERENCES
487

488 Tuka Al Hanai, Mohammad M Ghassemi, and James R Glass. Detecting depression with audio/text
489 sequence modeling of interviews. In *Interspeech*, pp. 1716–1720, 2018.

490 Davide Caffagni, Federico Cocchi, Luca Barsellotti, Nicholas Moratelli, Sara Sarto, Lorenzo
491 Baraldi, Marcella Cornia, and Rita Cucchiara. The revolution of multimodal large language mod-
492 els: a survey. *arXiv preprint arXiv:2402.12451*, 2024.

493 Edward L Campbell, Laura Docio-Fernández, Nicholas Cummins, and Carmen García-Mateo.
494 Speech and text processing for major depressive disorder detection. *Training*, 31:76, 2022.

495 Weidong Chen, Xiaofen Xing, Xiangmin Xu, Jianxin Pang, and Lan Du. Speechformer: A hierar-
496 chical efficient framework incorporating the characteristics of speech. In *Proc. Interspeech 2022*,
497 pp. 346–350, 2022.

498 Weidong Chen, Xiaofen Xing, Xiangmin Xu, Jianxin Pang, and Lan Du. Speechformer++: A hi-
499 erarchical efficient framework for paralinguistic speech processing. *IEEE/ACM Transactions on
500 Audio, Speech, and Language Processing*, 31:775–788, 2023.

501 Yunfei Chu, Jin Xu, Qian Yang, Haojie Wei, Xipin Wei, Zhifang Guo, Yichong Leng, Yuanjun Lv,
502 Jinzheng He, Junyang Lin, et al. Qwen2-audio technical report. *arXiv preprint arXiv:2407.10759*,
503 2024.

504 Wenliang Dai, Junnan Li, Dongxu Li, Anthony Tiong, Junqi Zhao, Weisheng Wang, Boyang Li,
505 Pascale Fung, and Steven Hoi. InstructBLIP: Towards general-purpose vision-language models
506 with instruction tuning. In *Thirty-seventh Conference on Neural Information Processing Systems*,
507 2023. URL <https://openreview.net/forum?id=vvoWPYqZJA>.

508 Tim Dettmers, Artidoro Pagnoni, Ari Holtzman, and Luke Zettlemoyer. Qlora: Efficient finetuning
509 of quantized llms. *Advances in neural information processing systems*, 36:10088–10115, 2023.

510 Ding Ding, Zeqian Ju, Yichong Leng, Songxiang Liu, Tong Liu, Zeyu Shang, Kai Shen, Wei Song,
511 Xu Tan, Heyi Tang, et al. Kimi-audio technical report. *arXiv preprint arXiv:2504.18425*, 2025.

512 Jonathan Gratch, Ron Artstein, Gale M Lucas, Giota Stratou, Stefan Scherer, Angela Nazarian,
513 Rachel Wood, Jill Boberg, David DeVault, Stacy Marsella, et al. The distress analysis interview
514 corpus of human and computer interviews. In *LREC*, volume 14, pp. 3123–3128. Reykjavik,
515 2014.

516 Yanrong Guo, Chenyang Zhu, Shijie Hao, and Richang Hong. A topic-attentive transformer-based
517 model for multimodal depression detection. *arXiv preprint arXiv:2206.13256*, 2022.

518 Albert Haque, Michelle Guo, Adam S Miner, and Li Fei-Fei. Measuring depression symptom sever-
519 ity from spoken language and 3d facial expressions. *arXiv preprint arXiv:1811.08592*, 2018.

520 Kaiming He, Xinlei Chen, Saining Xie, Yanghao Li, Piotr Dollár, and Ross Girshick. Masked au-
521 toencoders are scalable vision learners. In *Proceedings of the IEEE/CVF conference on computer
522 vision and pattern recognition*, pp. 16000–16009, 2022.

523 Amey Hengle, Atharva Kulkarni, Shantanu Patankar, Madhumitha Chandrasekaran, Sneha D’silva,
524 Jemima Jacob, and Rashmi Gupta. Still not quite there! evaluating large language models for
525 comorbid mental health diagnosis. In *Proceedings of the 2024 Conference on Empirical Methods
526 in Natural Language Processing*, pp. 16698–16721, 2024.

527 Edward J Hu, Yelong Shen, Phillip Wallis, Zeyuan Allen-Zhu, Yuanzhi Li, Shean Wang, Lu Wang,
528 Weizhu Chen, et al. Lora: Low-rank adaptation of large language models. *ICLR*, 1(2):3, 2022.

529 Juho Jung, Chaewon Kang, Jeewoo Yoon, Seungbae Kim, and Jinyoung Han. Hique: Hierarchical
530 question embedding network for multimodal depression detection. In *Proceedings of the 33rd
531 ACM International Conference on Information and Knowledge Management*, pp. 1049–1059,
532 2024.

540 Ah Young Kim, Eun Hye Jang, Seung-Hwan Lee, Kwang-Yeon Choi, Jeon Gue Park, and Hyun-
 541 Chool Shin. Automatic depression detection using smartphone-based text-dependent speech sig-
 542 nals: deep convolutional neural network approach. *Journal of medical Internet research*, 25:
 543 e34474, 2023.

544 Sanne Koops, Sanne G Brederoo, Janna N de Boer, Femke G Nadema, Alban E Voppel, and Iris E
 545 Sommer. Speech as a biomarker for depression. *CNS & Neurological Disorders-Drug Targets-
 546 CNS & Neurological Disorders*, 22(2):152–160, 2023.

547 Fernando C Krause, Eftihia Linardatos, David M Fresco, and Michael T Moore. Facial emotion
 548 recognition in major depressive disorder: A meta-analytic review. *Journal of affective disorders*,
 549 293:320–328, 2021.

550 Haotian Liu, Chunyuan Li, Qingyang Wu, and Yong Jae Lee. Visual instruction tuning. *Advances
 551 in neural information processing systems*, 36:34892–34916, 2023a.

552 June M Liu, Donghao Li, He Cao, Tianhe Ren, Zeyi Liao, and Jiamin Wu. Chatcounselor: A large
 553 language models for mental health support. *arXiv preprint arXiv:2309.15461*, 2023b.

554 Ilya Loshchilov and Frank Hutter. Decoupled weight decay regularization. *arXiv preprint
 555 arXiv:1711.05101*, 2017.

556 Haoyu Lu, Wen Liu, Bo Zhang, Bingxuan Wang, Kai Dong, Bo Liu, Jingxiang Sun, Tongzheng Ren,
 557 Zhusuo Li, Hao Yang, et al. Deepseek-vl: towards real-world vision-language understanding.
 558 *arXiv preprint arXiv:2403.05525*, 2024.

559 Humza Naveed, Asad Ullah Khan, Shi Qiu, Muhammad Saqib, Saeed Anwar, Muhammad Usman,
 560 Naveed Akhtar, Nick Barnes, and Ajmal Mian. A comprehensive overview of large language
 561 models. *arXiv preprint arXiv:2307.06435*, 2023.

562 Alice Othmani, Daoud Kadoch, Kamil Bentounes, Emna Rejaibi, Romain Alfred, and Abdenour
 563 Hadid. Towards robust deep neural networks for affect and depression recognition from speech.
 564 In *International conference on pattern recognition*, pp. 5–19. Springer, 2021.

565 John E Perez and Ronald E Riggio. Nonverbal social skills and psychopathology. *Nonverbal behav-
 566 ior in clinical settings*, pp. 17–44, 2003.

567 Rafał Poświata and Michał Perelkiewicz. OPI@LT-EDI-ACL2022: Detecting signs of depres-
 568 sion from social media text using RoBERTa pre-trained language models. In Bharathi Raja
 569 Chakravarthi, B Bharathi, John P McCrae, Manel Zarrouk, Kalika Bali, and Paul Buitelaar (eds.),
 570 *Proceedings of the Second Workshop on Language Technology for Equality, Diversity and Inclu-
 571 sion*, pp. 276–282, Dublin, Ireland, May 2022. Association for Computational Linguistics. doi:
 572 10.18653/v1/2022.ltedi-1.40. URL <https://aclanthology.org/2022.ltedi-1.40/>.

573 Qwen, :, An Yang, Baosong Yang, Beichen Zhang, Binyuan Hui, Bo Zheng, Bowen Yu, Chengyuan
 574 Li, Dayiheng Liu, Fei Huang, Haoran Wei, Huan Lin, Jian Yang, Jianhong Tu, Jianwei Zhang,
 575 Jianxin Yang, Jiaxi Yang, Jingren Zhou, Junyang Lin, Kai Dang, Keming Lu, Keqin Bao, Kexin
 576 Yang, Le Yu, Mei Li, Mingfeng Xue, Pei Zhang, Qin Zhu, Rui Men, Runji Lin, Tianhao Li, Tianyi
 577 Tang, Tingyu Xia, Xingzhang Ren, Xuancheng Ren, Yang Fan, Yang Su, Yichang Zhang, Yu Wan,
 578 Yuqiong Liu, Zeyu Cui, Zhenru Zhang, and Zihan Qiu. Qwen2.5 technical report, 2025. URL
 579 <https://arxiv.org/abs/2412.15115>.

580 Alec Radford, Jong Wook Kim, Tao Xu, Greg Brockman, Christine McLeavey, and Ilya Sutskever.
 581 Robust speech recognition via large-scale weak supervision. In *International conference on ma-
 582 chine learning*, pp. 28492–28518. PMLR, 2023.

583 Misha Sadeghi, Robert Richer, Bernhard Egger, Lena Schindler-Gmelch, Lydia Helene Rupp, Far-
 584 naz Rahimi, Matthias Berking, and Bjoern M Eskofier. Harnessing multimodal approaches for
 585 depression detection using large language models and facial expressions. *npj Mental Health Re-
 586 search*, 3(1):66, 2024.

587 Zixuan Shangguan, Zhenyu Liu, Gang Li, Qiongqiong Chen, Zhijie Ding, and Bin Hu. Dual-stream
 588 multiple instance learning for depression detection with facial expression videos. *IEEE Transac-
 589 tions on Neural Systems and Rehabilitation Engineering*, 31:554–563, 2022.

594 Ying Shen, Huiyu Yang, and Lin Lin. Automatic depression detection: An emotional audio-textual
 595 corpus and a gru/bilstm-based model. In *ICASSP 2022-2022 IEEE International Conference on*
 596 *Acoustics, Speech and Signal Processing (ICASSP)*, pp. 6247–6251. IEEE, 2022.

597

598 Aleks Stolicyn, J Douglas Steele, and Peggy Seriès. Prediction of depression symptoms in individual
 599 subjects with face and eye movement tracking. *Psychological medicine*, 52(9):1784–1792, 2022.

600

601 Anita Thapar, Olga Eyre, Vikram Patel, and David Brent. Depression in young people. *The Lancet*,
 602 400(10352):617–631, 2022.

603

604 Ermal Toto, ML Tlachac, and Elke A Rundensteiner. Audibert: A deep transfer learning multimodal
 605 classification framework for depression screening. In *Proceedings of the 30th ACM international*
 606 *conference on information & knowledge management*, pp. 4145–4154, 2021.

607

608 Hugo Touvron, Louis Martin, Kevin Stone, Peter Albert, Amjad Almahairi, Yasmine Babaei, Niko-
 609 lay Bashlykov, Soumya Batra, Prajjwal Bhargava, Shruti Bhosale, et al. Llama 2: Open foundation
 610 and fine-tuned chat models. *arXiv preprint arXiv:2307.09288*, 2023.

611

612 Peng Wang, Shuai Bai, Sinan Tan, Shijie Wang, Zhihao Fan, Jinze Bai, Keqin Chen, Xuejing Liu,
 613 Jialin Wang, Wenbin Ge, et al. Qwen2-vl: Enhancing vision-language model’s perception of the
 614 world at any resolution. *arXiv preprint arXiv:2409.12191*, 2024.

615

616 Peter Waxer. Nonverbal cues for depression. *Journal of Abnormal Psychology*, 83(3):319, 1974.

617

618 Ping-Cheng Wei, Kunyu Peng, Alina Roitberg, Kailun Yang, Jiaming Zhang, and Rainer Stiefelha-
 619 gen. Multi-modal depression estimation based on sub-attentional fusion. In *European Conference*
 620 *on Computer Vision*, pp. 623–639. Springer, 2022.

621

622 James R Williamson, Elizabeth Godoy, Miriam Cha, Adrienne Schwarzenbuber, Pooya Khorrami,
 623 Youngjune Gwon, Hsiang-Tsung Kung, Charlie Dagli, and Thomas F Quatieri. Detecting depres-
 624 sion using vocal, facial and semantic communication cues. In *Proceedings of the 6th international*
 625 *workshop on audio/visual emotion challenge*, pp. 11–18, 2016.

626

627 Wen Wu, Chao Zhang, and Philip C Woodland. Self-supervised representations in speech-based
 628 depression detection. In *ICASSP 2023-2023 IEEE International Conference on Acoustics, Speech*
 629 *and Signal Processing (ICASSP)*, pp. 1–5. IEEE, 2023.

630

631 Jin Xu, Zhifang Guo, Jinzheng He, Hangrui Hu, Ting He, Shuai Bai, Keqin Chen, Jialin Wang, Yang
 632 Fan, Kai Dang, et al. Qwen2. 5-omni technical report. *arXiv preprint arXiv:2503.20215*, 2025.

633

634 Xuhai Xu, Bingsheng Yao, Yuanzhe Dong, Saadia Gabriel, Hong Yu, James Hendler, Marzyeh Ghas-
 635 semi, Anind K Dey, and Dakuo Wang. Mental-llm: Leveraging large language models for mental
 636 health prediction via online text data. *Proceedings of the ACM on Interactive, Mobile, Wearable*
 637 *and Ubiquitous Technologies*, 8(1):1–32, 2024.

638

639 Junqi Xue, Ruihan Qin, Xinxu Zhou, Honghai Liu, Min Zhang, and Zhiguo Zhang. Fusing multi-
 640 level features from audio and contextual sentence embedding from text for interview-based de-
 641 pression detection. In *ICASSP 2024-2024 IEEE International Conference on Acoustics, Speech*
 642 *and Signal Processing (ICASSP)*, pp. 6790–6794. IEEE, 2024.

643

644 An Yang, Baosong Yang, Binyuan Hui, Bo Zheng, Bowen Yu, Chang Zhou, Chengping Li,
 645 Chengyuan Li, Dayiheng Liu, Fei Huang, Guanting Dong, et al. Qwen2 technical report. *arXiv*
 646 *preprint arXiv:2407.10671*, 2024.

647

648 Duzhen Zhang, Yahan Yu, Jiahua Dong, Chenxing Li, Dan Su, Chenhui Chu, and Dong Yu. Mm-
 649 llms: Recent advances in multimodal large language models. *arXiv preprint arXiv:2401.13601*,
 650 2024a.

651

652 Xiangyu Zhang, Hexin Liu, Kaishuai Xu, Qiquan Zhang, Daijiao Liu, Beena Ahmed, and Julien
 653 Epps. When llms meets acoustic landmarks: An efficient approach to integrate speech into large
 654 language models for depression detection. In *Proceedings of the 2024 Conference on Empirical*
 655 *Methods in Natural Language Processing*, pp. 146–158, 2024b.

648 Zhenwei Zhang, Shengming Zhang, Dong Ni, Zhaoguo Wei, Kongjun Yang, Shan Jin, Gan Huang,
 649 Zhen Liang, Li Zhang, Linling Li, et al. Multimodal sensing for depression risk detection: Inte-
 650 grating audio, video, and text data. *Sensors*, 24(12):3714, 2024c.
 651

652 Zhiguo Zheng, Lijuan Liang, Xiong Luo, Jie Chen, Meirong Lin, Guanjun Wang, and Chenyang
 653 Xue. Diagnosing and tracking depression based on eye movement in response to virtual reality.
 654 *Frontiers in Psychiatry*, 15:1280935, 2024.

655 Deyao Zhu, Jun Chen, Xiaoqian Shen, Xiang Li, and Mohamed Elhoseiny. Minigpt-4: En-
 656 hancing vision-language understanding with advanced large language models. *arXiv preprint*
 657 *arXiv:2304.10592*, 2023.
 658

660 A IMPLEMENTATION DETAILS

661 Our framework is implemented using the HuggingFace *transformers* library with PyTorch 2.1. The
 662 full hyperparameter configurations used during training are summarized in Table 4. We adopt the
 663 AdamW optimizer (Loshchilov & Hutter, 2017) for model optimization. To improve training speed
 664 without compromising performance, we enable TensorFloat32 (TF32) computation and apply auto-
 665 matic mixed-precision training using BFloat16 (BF16). For parameter-efficient fine-tuning (PEFT)
 666 of the Qwen2-Audio model on the depression detection task, we employ QLoRA (Dettmers et al.,
 667 2023), which compresses the base model to 4-bit precision to reduce memory usage and improve
 668 computational efficiency. The full training process requires approximately 90+ GPU hours on an
 669 NVIDIA H200 141GB GPU. This includes around 40 hours for self-supervised visual pretraining,
 670 20 hours for utterance-level audio-visual alignment, and 30 hours for multimodal instruction tuning.
 671 Early stopping is applied in all stages when training loss plateaus.
 672

	Stage I	Stage II	Stage III
Optimizer		AdamW	
Learning Rate	1.5e-4	1e-6	3e-6
β_1		0.9	
β_2	0.95		0.999
Weight Decay	0		0.001
Batch Size	128	64	8
Grad Accum Steps	8	16	8
Scheduler		Cosine LR	
Num Epochs	50	20	3
Warm Up Epochs	5	2	0.1
Max Grad Norm	1.0		0.5
BF16		True	
TF32		True	

687 Table 4: Training hyperparameters.
 688
 689

690 B DETAILS OF TIMESTAMP-SYNCHRONIZED DATA AUGMENTATION

691 Following the approach of Wu et al. (2023), we generate subdialogues from the original interview
 692 transcripts to mitigate class imbalance and expand the size of the training set. In our data augmenta-
 693 tion pipeline, we enforce strict synchronization among transcripts, audio, and video to ensure precise
 694 timestamp-level alignment. However, due to varying frame rates across modalities, achieving syn-
 695 chronization presents a technical challenge. For example, audio recordings are typically captured at
 696 a 16,000 Hz sampling rate and later converted into Mel-spectrograms with a frame rate of 100 Hz,
 697 while video recordings are collected at 30 frames per second (FPS). To address this discrepancy,
 698 we constrain the start and end timestamps of each subdialogue to align with whole seconds (i.e.,
 699 integer-second boundaries).

700 Additionally, we require each subdialogue to begin with an utterance from the interviewer and con-
 701 clude with a response from the participant. This design choice ensures that each subdialogue forms

702 **Algorithm 1** Time-Sync Data Augmentation

703

```

704 1:  $N^+$   $\leftarrow$  Number of positive samples in the training set
705 2:  $N^-$   $\leftarrow$  Number of negative samples in the training set
706 3: Set number of subdialogues per positive sample  $M^+$ 
707 4: Set minimum length of subdialogue in seconds  $d_{min}$ 
708 5: Set maximum length of subdialogue in seconds  $d_{max}$ 
709 6:  $M^- = N^-/N^+ \times M^+ \leftarrow$  Number of sub-dialogues per negative sample
710 7: for Dialogue  $X^{(n)} = (T^n, A^n, V^n), n = 1, 2, \dots, N$  do
711 8:    $D \leftarrow$  Dialogue length in seconds
712 9:    $\{\varepsilon_i\} \leftarrow$  Interviewer utterance start timestamps
713 10:   $\{\varepsilon_p\} \leftarrow$  Participant utterance end timestamps
714 11:  if  $X^{(n)}$  is positive then
715 12:     $M \leftarrow M^+$ 
716 13:  else
717 14:     $M \leftarrow M^-$ 
718 15:  end if
719 16:  for Sub-dialogue  $X^{(n)m}, m = 1$  to  $M$  do
720 17:    Sample length  $d$  uniformly from  $(d_{min}, d_{max})$ 
721 18:    Sample start timestamp  $\varepsilon'_s \in \{\varepsilon_i\}$  from range  $(0, D - d)$ 
722 19:    Round the start timestamp to its closest integer second  $\varepsilon_s \leftarrow \lfloor \varepsilon'_s \rfloor$ 
723 20:     $\varepsilon_{tmp} = \varepsilon_s + d \leftarrow$  Raw end timestamp
724 21:    Sample end timestamp  $\varepsilon'_e \in \{\varepsilon_p\}$  and  $\min |\varepsilon'_e - \varepsilon_{tmp}|$ 
725 22:    Round the end timestamp to its closest integer second  $\varepsilon_e \leftarrow \lceil \varepsilon'_e \rceil$ 
726 23:    Generate subdialogue  $T^{(n)m} \leftarrow T_{\varepsilon_s:\varepsilon_e}^{(n)}$ 
727 24:    Obtain the raw audio segment  $A'^{(n)m} \leftarrow A_{\varepsilon_s:\varepsilon_e}^{(n)}$ 
728 25:    Obtain the raw visual segment  $V'^{(n)m} \leftarrow V_{\varepsilon_s:\varepsilon_e}^{(n)}$ 
729 26:    Remove the interviewer utterances  $A^{(n)m} \leftarrow A'^{(n)m}$  and  $V^{(n)m} \leftarrow V'^{(n)m}$ 
730 27:    Subdialogue  $X^{(n)m} = (T^{(n)m}, A^{(n)m}, V^{(n)m})$ 
731 28:  end for
732 29: end for

```

731 a complete and contextually coherent conversational unit, with a clear initiation and response structure. Such a constraint preserves the semantic continuity and logical flow within each segment, 732 making them more suitable for downstream tasks that rely on natural discourse patterns. Moreover, 733 this structure aligns with the training paradigm of large language models, which are typically 734 pre-trained on large-scale dialogue corpora. By maintaining this dialogue consistency, we enhance the 735 model’s ability to interpret the subdialogues effectively within a familiar conversational framework. 736

737 **C THE PROMPT DESIGN FOR INSTRUCTION TUNING**

739 During instruction tuning, we design a system prompt to guide the behavior of the language model. 740 Given that the Qwen2-Audio-Instruct model has been fine-tuned on audio analysis tasks, we adopt 741 a chat-based prompt template to elicit model responses. Notably, we use the same prompt design 742 for both the Qwen2-Audio family and our multi-modal LLM. This consistency is based on our 743 integration strategy, where visual embeddings are directly added to the audio embeddings without 744 modifying the model architecture. Therefore, we assume that the model can still function effectively 745 even without explicitly referencing visual information in the prompt. 746

747 **System Prompt** Below is a conversation between an interviewer and a 748 participant. Please analyze the transcripts and audio, and find 749 whether the participant is affected by depression. 750

751 **Instructions** Audio: {audio} \n Interview conversation: {transcripts} 752 \n Response: \n

753
754
755